

Article

PM₁₀ Chemical Profile during North African Dust Episodes over French West Indies

Philippe Quénel ^{1,*}, Jade Vadel ^{1,2}, Céline Garbin ³, Séverine Durand ¹, Olivier Favez ^{4,5}, Alexandre Albinet ^{4,5}, Christina Raghoundan ³, Stéphanie Guyomard ⁶, Laurent Yves Alleman ^{5,7}, and Fabien Mercier ¹

- ¹ Irset (Institut de Recherche en Santé, Environnement et Travail)—UMR_S 1085, University Rennes, Inserm, EHESP, 35000 Rennes, France; jade.vadel@orange.fr (J.V.); severine.durand@ehesp.fr (S.D.); Fabien.Mercier@ehesp.fr (F.M.)
- ² ENSAI, 35170 Bruz, France
- ³ Gwad'Air-Air Quality Monitoring Agency, 97170 Petit-Bourg, France; c.garbin@gwadair.fr (C.G.); c.ragh@gwadair.fr (C.R.)
- ⁴ Ineris, 60560 Verneuil en Halatte, France; olivier.favez@ineris.fr (O.F.); alexandre.albinet@ineris.fr (A.A.)
- ⁵ LCSQA, 60560 Verneuil en Halatte, France; laurent.alleman@imt-lille-douai.fr
- ⁶ Unité Transmission Réservoir et Diversité des Pathogènes, Institut Pasteur de Guadeloupe, Les Abymes, 97139 Guadeloupe, France; sguyomard@pasteur-guadeloupe.fr
- ⁷ IMT Lille Douai, Institut Mines-Télécom, Center for Energy and Environment, University Lille, 59500 Lille, France
- * Correspondence: philippe.quenel@ehesp.fr; Tel.: +33-680-244-023



Citation: Quénel, P.; Vadel, J.; Garbin, C.; Durand, S.; Favez, O.; Albinet, A.; Raghoundan, C.; Guyomard, S.; Alleman, L.Y.; Mercier, F. PM₁₀ Chemical Profile during North African Dust Episodes over French West Indies. *Atmosphere* **2021**, *12*, 277. <https://doi.org/10.3390/atmos12020277>

Academic Editors: Olivier Delhomme, Prashant Kumar and Antonio Donato
Received: 7 December 2020
Accepted: 11 February 2021
Published: 19 February 2021

Publisher's Note: MDPI stays neutral with regard to jurisdictional claims in published maps and institutional affiliations.



Copyright: © 2021 by the authors. Licensee MDPI, Basel, Switzerland. This article is an open access article distributed under the terms and conditions of the Creative Commons Attribution (CC BY) license (<https://creativecommons.org/licenses/by/4.0/>).

Abstract: The French West Indies are periodically affected by North African dust episodes (NADE) resulting in PM₁₀ concentrations exceeding air quality standards. The aim of the present study was to decipher the PM₁₀ chemical profile during NADE over Guadeloupe. PM₁₀ samples were collected daily at a rural site and an urban site during five episodes between April and October in 2017. During these events, the median PM₁₀ mass concentrations were, on average, 2 to 5 times higher than in the post-episode baseline period. Sampled filters were analyzed for their quantification of chemical constituents including carbonaceous fractions (elemental and organic carbon, EC/OC), anions/cations and levoglucosan, 51 elements, and 57 selected organic species. An orthogonal partial least squares discriminant analysis (OPLS-DA) was conducted to identify the specific chemical profile of PM₁₀ during NADE: 16 elements were identified as the most discriminant between the NADE and the control samples with mass concentration levels twice as high during a NADE. Among them, only two (Mn and V) are classified as emerging pollutant while no limit values exist for the other ones. The extensive characterization of the NADE PM₁₀ chemical profile we performed is a key step to assess the chemical exposure of French West Indies populations during such events.

Keywords: chemical composition; exposure; French West Indies; metals; PM₁₀; North African dust

1. Introduction

As their neighboring countries, the French West Indies are periodically affected by African dust episodes (ADE) from northern Africa or western Africa [1]. These can last several consecutive days, occurring mainly between March and October, and resulting in ambient particles concentrations exceeding the PM₁₀ EU air quality standards [2].

The meteorological mechanism of this phenomenon is well known. When the Inter-Tropical Convergence Zone is installed, the warm air masses of the northern and southern hemispheres converge and rise in altitude (typically up to 5–7 km), carrying desert dust particles over long distances across the Atlantic Ocean with the trade winds (1.5 to 3.7 km in height) and reaching the Caribbean one to two weeks after leaving the African coast [3–6]. Some of these particles deposit during the transport, but the convection of the lower atmospheric layers is sufficient to maintain a significant quantity of them above the trade wind.

These events have substantial impact on the global climate (through direct and indirect radiative forcing), on marine productivity and terrestrial ecosystems as well as on human health [7,8]. In particular, the health hazards associated with aerosols exposure depend on the size of the particles, on their chemical composition and microbiological agents adsorbed on their surface. Particles with a median aerodynamic diameter $\leq 10 \mu\text{m}$ (PM_{10}) are the most likely deposited in the bronchi and thus affecting respiratory tract (bronchitis, asthma, chronic obstructive pulmonary disease, etc.), while fine particles with an aerodynamic diameter $\leq 2.5 \mu\text{m}$ ($\text{PM}_{2.5}$) are more likely to reach the pulmonary alveoli, causing systemic inflammation leading to cardiovascular effects [9].

Numerous studies carried out in the Mediterranean region found an association between PM from African dust and daily mortality for cardiovascular, respiratory, or cerebrovascular causes. The impacts of ADE on cardiorespiratory mortality and morbidity have been estimated of the same order of magnitude as of atmospheric suspended particles in general [10,11], or higher as a result of a modifying effect of ADE on mortality risk related to PM_{10} [12–16]. However, the associations observed with PM_{10} or $\text{PM}_{10-2.5}$ vary widely from one study to another and from one region to another, highlighting the need for a chemical characterization of these particles and ADE source-health studies [17]. For instance, in the Caribbean basin, some studies conducted in Barbados did not show any significant link between North African dust episodes (NADE) and pediatric hospital visits for asthma [18], while in Trinidad, a relationship has been observed with pediatric emergency room admissions for asthma [19]. In the French West Indies, a study conducted in Martinique reported an increased risk of hospitalization for cardiovascular or respiratory causes during NADE [20], and in Guadeloupe, NADE were associated with an increased risk of pediatric emergency room visits for asthma crisis [21]. In these studies, the exposure to NADE was estimated from mass concentrations of PM_{10} and/or $\text{PM}_{2.5}$, but none of them investigated the chemical composition of these particles. Several studies carried out in the Mediterranean basin have addressed the chemical characterization of African dust particles [12,22,23], but only one environmental study has been conducted in the Caribbean (U.S. Virgin Islands and Trinidad and Tobago) reporting the content of metals and several organic species—including organochlorine and organophosphorus pesticides, polycyclic aromatic hydrocarbons (PAHs), and polychlorinated biphenyls (PCBs)—within NADE total suspended particles (TSP) [24].

Recently, epidemiological studies have identified exposure during pregnancy to metalloids or metals, such as arsenic, cadmium, and lead, as a risk factor for fetal growth [25–31]. Similar findings were published for some semi volatile organic compounds (SVOCs) such as phthalates including di(2-ethylhexyl)phthalate (DEHP) and diisononylphthalate (DiNP) [32,33], organophosphorus, organochlorine, or triazine pesticides [27,34–37], and PCBs [28,38]. Furthermore, as high rates of largely unexplained adverse pregnancy outcomes are observed in the French West Indies [39], we retrospectively exploited data from a mother–child cohort conducted in Guadeloupe to evaluate the association between mother’s exposure during pregnancy to NADE PM_{10} and pre-term birth. Obtained results have shown an association with an increase in relative risk with the levels of PM_{10} and the frequency of intense NADE [40]. The aim of the present study was to decipher the exposure of the Guadeloupean population to chemical compounds and microbiological agents of PM_{10} related to NADE. This manuscript is then presented and discusses the extended chemical profile of NADE PM_{10} samples collected in Guadeloupe both in terms of emission sources and potential health impact.

2. Experiments

2.1. Samplings

Filter samples were collected on pure quartz fiber filters (150 mm diameter, TisuQuartz, Pallflex)—preconditioned at $500 \text{ }^\circ\text{C}$ for 2 h—using a DA80 Digital high volume sampler, at a flow rate of $30 \text{ m}^3/\text{h}$. The filter collection was decided based on the forecasts from the Navy Aerosol Analysis and Prediction System Global Aerosol Model [41] which

made possible to anticipate 48–72 h in advance the occurrence and expected intensity of NADE.

These samples were taken: (i) at Anse-Bertrand in a rural area on the East windward coast, by a sampler located in accordance with the protocol of the European Directive 2008/50/EC on ambient air quality [42], away from the sea and any anthropogenic activity (WGS84: Longitude = -61.5281492 , Latitude = 16.2330264), and (ii) at a urban background site representative of the Pointe-à-Pitre air quality (i.e., located relatively far from any road traffic or other local sources (WGS84: Longitude = -61.4275882 , Latitude = 16.4517761) (Figure 1).

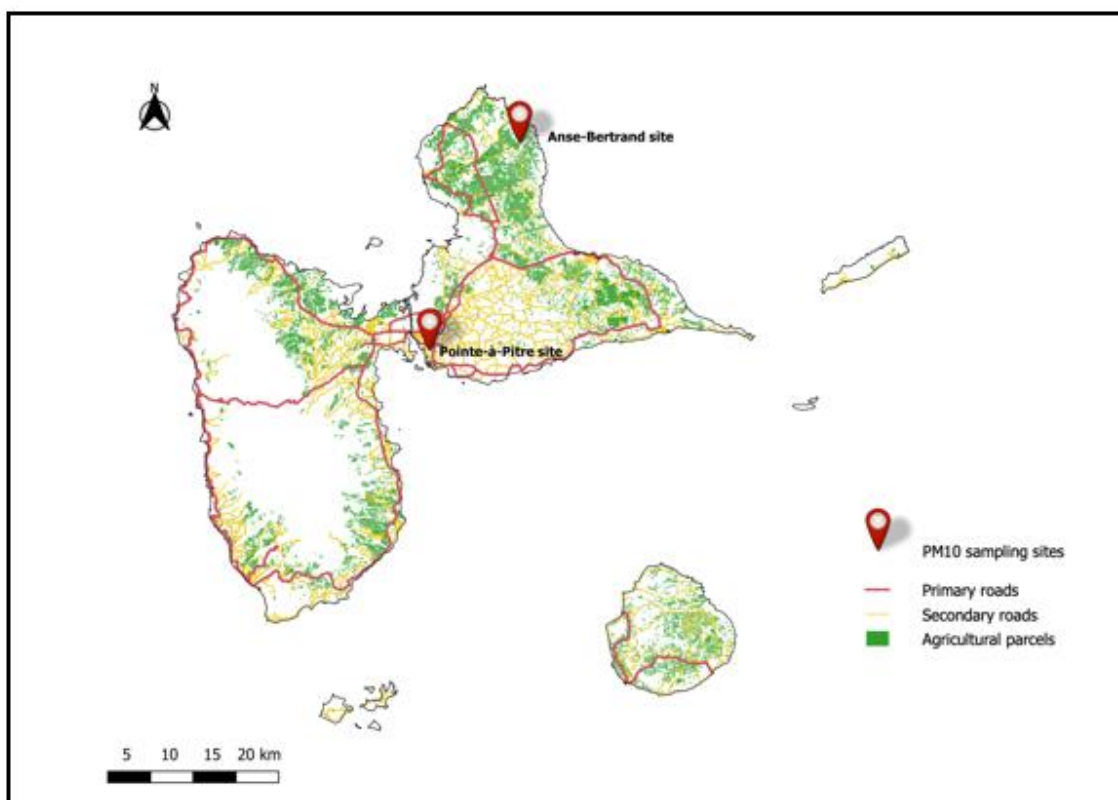


Figure 1. Geographical position of the collectors for NADE dust sampling, Guadeloupe. (Source Gwad’Air).

Between March and November 2017, 5 periods of NADE occurring in Guadeloupe were sampled for PM_{10} (Table 1). In total, 27 samples were collected daily (from midnight to midnight) during ($n = 20$) and after ($n = 7$) each NADE period (control sample—CS) (Table 1). Of the 20 samples collected during NADE, 10 were collected in the urban area and 10 in the rural area. Of the 7 CS, 2 were collected in the urban area and 5 in the rural area. For quality control purpose, 6 field blanks and 5 laboratory blanks were included to the sample matrices. Field blanks are blank filters that were subjected to the same procedure as an actual sample, except that they have not been exposed to sampling. They reflect both media contamination, contamination on site during the sampling, handling and transport periods, and contamination related to storage before and after sampling. Laboratory blanks are unsampled blank filters that do not leave the laboratory storage site during the entire period of outdoor sampling. Placed in aluminum foil, they have been stored in a desiccator. They were then analyzed according to the same analytical procedure as the actual samples, in order to isolate any specific problem on the measurement chain.

Table 1. Periods and number of PM₁₀ samples collected in rural and urban area, Guadeloupe, March—November 2017.

Start Date (mm/dd/yy)	End Date (mm/dd/yy)	Number of Samples Collected during NADE	Number of Control Samples Collected Just after NADE
Urban area			
04/02/17	04/05/17	1	1
05/19/17	05/30/17	9	1
Rural area			
06/26/17	06/28/17	2	2
09/25/17	09/28/17	2	2
10/15/17	10/24/17	6	1 *

* re-qualified as NADE (see Section 3.4).

After sampling, the filters were wrapped in aluminum foil, placed in sealed polyethylene bags, and stored at $-20\text{ }^{\circ}\text{C}$. Shipment of these samples to mainland France for chemical analyses was achieved by express delivery services (48–72 h) in temperature-controlled packages ($<5\text{ }^{\circ}\text{C}$).

Furthermore, automated co-located PM₁₀ mass concentration measurements have been obtained using Tapered Element Oscillating Microbalances equipped with Filter Dynamics Measurement Systems (Thermo, TEOM-FDMS) in compliance with the relevant EN 16450 EU standard [43].

2.2. Chemical Species Analyses

Sampled filters were subjected to various chemical analyses for the quantification of the major chemical constituents and trace compounds as described hereafter.

2.2.1. Carbonaceous Aerosols

The carbonaceous fractions—i.e., organic carbon (OC) and elemental carbon (EC)—were analyzed on 1.5 cm^2 punches using a Sunset Lab. analyzer [44] and following the EUSAAR2 thermo-optical protocol [45].

2.2.2. Anions, Cations and Levoglucosan

Major water-soluble inorganic species—namely NH_4^+ , Na^+ , K^+ , Mg^{2+} , and Ca^{2+} for cations, as well as Cl^- , NO_3^- , and SO_4^{2-} for anions—were analyzed using ion chromatography (IC). Prior to analysis, 1.5 cm^2 punches were soaked for 30 min in ultra-pure water and obtained solutions were then filtered using $0.25\text{ }\mu\text{m}$ porosity filters. The same solutions were also used for the quantification of levoglucosan—commonly used as a marker for biomass burning aerosols—using IC device equipped with amperometric detector. Detailed analytical procedures used for these measurements can be found in Waked et al. [46].

2.2.3. Metals and Metalloids

Punches of 4.7 cm diameter were used to measure a first set of elements based on the ambient air quality EN14902:2005 standard [47]. These elements included Ag, Al, As, B, Ba, Be, Bi, Ca, Cd, Ce, Co, Cr, Cs, Cu, Fe, Hg, K, La, Li, Mg, Mn, Mo, Na, Ni, Pb, Rb, Ru, Sc, Se, Sn, Sr, Tl, Th, Ti, U, and V. The analysis [48,49] were performed on a Perkin Elmer NexION 300× inductively coupled plasma mass spectrometer (ICP–MS). Prior to analyses, each sub-sample was acid digested (HNO_3 : 2 mL; H_2O_2 : 1 mL) at $220\text{ }^{\circ}\text{C}$ in a microwave oven (Ultrawave, Thermo-Scientific). Due to the quartz content of the filter medium, HF was not included in the mineralization procedure and Si was not analyzed. The digests were diluted to a final volume of 50 mL using ultrapure water and stored at $4\text{ }^{\circ}\text{C}$ until analyses. Each sample was analyzed in triplicates in order to estimate the repeatability of the technique. We performed several measurements of reagent blanks and quality control (QC) standard solutions attached to the NIST for analytical validation. Mean filter blank values were subtracted to the elemental concentrations. Internal standards

(⁶⁹Ga, ¹⁰³Rh) were added (1 µg L⁻¹) to all analyzed solutions to correct the drift of the ICP-MS signal. In addition, 10 samples (about 1 mg) of NIST SRM 1648a (Urban particulate matter) were systematically tested as standard reference material to validate the whole extraction procedure. Most of the measured elements were validated with a recovery rate ranging between 85% and 110%, except for refractory elements like Al (65%), K (64%), La (70%), Th (66%), or Ti (63%). The reported concentrations for these last elements take into account these lower recovery rates.

One 1/4 filter was used to achieve a second round of analyses to obtain concentrations of Sb, Dy, Er, Eu, Gd, Ho, Lu, Nd, Pr, Sm, Tb, Tm, Yb, Zn, and Zr. To do so, the extraction was carried out using a mixture of aqua regia (2.5 mL HNO₃; 5 mL HCl) at 150 °C with a microwave oven (Ethos 1 microwaves—Milestone). The digests were filtered and then adjusted to a final volume of 100 mL using ultra-pure water and stored at 4 °C until analyses. Samples were analyzed by an ICP-MS 7900 mass spectrometer (Agilent Technologies) in triplicates in order to estimate the repeatability of the technique and the RSD checked. Blanks and quality control (QC) standard solutions have been integrated for each analysis series. An internal standard mixture (⁷²Ge, ¹⁰³Rh, ¹¹⁵In, ¹⁸⁵Re, ¹⁹³Ir) was added, on-line, to all samples to correct for ICP-MS signal drift. Certified controls, CRM SS1, CRM SS2, and NIST SRM 1944 (two soils and 1 sediment) were systematically tested as reference materials to validate the digestion procedure (Table S1).

2.2.4. Organic Species

No gaseous phase having been collected during sampling, SVOC were analyzed from particulate phase only. Part of the filter was used to measure the mass concentrations of 20 PAHs in PM₁₀ following the EN 15549 and CEN/TS 16645 standard procedures and as reported previously [50]. These 20 PAHs include: 1-methylnaphthalene, 2-methylfluoranthene, 2-methylnaphthalene, acenaphthene, anthracene, benzo[a]anthracene, benzo[a]pyrene, benzo[b]-fluoranthene, benzo[e]pyrene, benzo[g,h,i]perylene, benzo[j]fluoranthene, benzo[k]fluoranthene, chrysene, coronene, dibenzo[a,h]anthracene, fluoranthene, fluorene, indeno[1,2,3-cd]pyrene, pyrene, and retene. Filters were extracted by pressurized liquid extraction (PLE) and analyses were performed by ultra-performance liquid chromatography with fluorescence detection (UPLC/Fluorescence).

Finally, another 1/4 filter was dedicated to the analysis of additional organic compounds known to be or to have been present in Guadeloupe, and/or that have been already detected in NADE particles in the Eastern Caribbean [24]. These are:

- 14 organochlorine pesticides: 2,4'-DDD, 2,4'-DDE, 2,4'-DDT, 4,4'-DDD, 4,4'-DDE, 4,4'-DDT, aldrin, alpha-endosulfan, alpha-HCH, beta-endosulfan, dieldrin, endosulfan sulfate, gamma-HCH (lindane), and hexachlorobenzene (HCB);
- 1 organophosphate: tributylphosphate (TBP);
- 3 organophosphorus pesticides: chlorpyrifos-ethyl, diazinon, and dichlorvos;
- 1 herbicide: oxadiazon;
- 5 pyrethroid pesticides: cyfluthrin, cypermethrin, deltamethrin, permethrin, and tetramethrin;
- 9 PCBs: PCB 28, 31, 52, 101, 105, 118, 138, 153, and 180;
- 4 phthalates: BBP, DBP, DEP, and DiNP.

Filters were extracted by pressurized liquid extraction (PLE) and analyses were performed by gas chromatography coupled with tandem mass spectrometry (GC/MS/MS). A detailed description of the analytical method including quality assurance and quality control has already been published [51,52]. Briefly, each batch included: (i) Up to 20 samples, (ii) nine calibration samples and one calibration blank sample to generate quadratic calibration curves intended for quantification, (iii) one procedural blank sample (pre-conditioned QFF quarter) to assess whether contamination may have occurred during analysis, and (iv) two procedural QC samples (pre-conditioned QFF quarter spiked at the QL level and at an intermediate level) analyzed as regular samples to check for method accuracy. Positive values for each substance were confirmed by comparing retention times and MRM transitions ratios between calibration samples and real samples. The data validation protocol

included several conditions: (i) The determination coefficient of the calibration curve had to be greater than 0.995, (ii) the response of a substance in the calibration blank sample and in the procedural blank samples had to be lower than 50% of that in the calibration sample at the QL level, and (iii) the concentration of a compound measured in the procedural QC samples had to be within $\pm 50\%$ of its theoretical concentration value for the QC sample at the QL level (QC1) and $\pm 30\%$ for the QC sample at an intermediate level (QC2). The QC results are presented in Table S2 in the Supplementary Material.

2.3. Data Treatment Procedures

2.3.1. Chemical Datasets

Due to very low concentrations (e.g., below detection limits), part of the investigated chemical compounds could not be used for data treatments. Species that could eventually be considered were selected on the basis of their quantification frequency ($Q_f = \text{number of samples with values} > \text{QL} / \text{number of samples analyzed}$), leading to the following classification:

- 45 compounds (35 elements, 1 organic, 8 anions-cations, organic carbon) with a $Q_f > 0.6$ have been selected for further analysis; the values below the quantification limit (QL) have been replaced by the corresponding value $QL/2$;
- 15 compounds (3 elements, 11 organic compounds, elemental carbon) quantified with Q_f between 0.3 and 0.6 were kept for qualitative analysis only (see below) and coded into binary variables (quantified/not quantified);
- 59 compounds (13 elements, 45 organics, 1 anion) with a $Q_f < 0.3$ were not retained for further data analysis.

2.3.2. Dust Episodes Origin

In order to document the origin of dust episodes, a weight of evidence approach was used based on the elemental ratios largely used in the literature [53–55] to estimate and compare chemical characteristics of different dust origins.

Elemental ratios (Ca/Al, Ti/Fe, Ti/Ca, Fe/Al, and (Ca+Mg)/Fe) were calculated for NADE samples; the confidence interval of the mean ratios being calculated from the Student's Law.

2.3.3. Chemical Characteristics of NADE PM₁₀

A descriptive analysis was performed on the data in volumetric concentration (ng/m^3) for PM₁₀, and in abundances ($\mu\text{g}/\text{g}$) for chemical compounds; the confidence interval of the means being calculated from the Student's *t*-test. Then, we conducted an analysis of the data based on the PM₁₀ chemical composition, using first an exploratory unsupervised approach in order to let the samples split up on their own into clusters. The description of the characteristic variables of each of the clusters provides a first picture of the chemical compounds discriminating between NADE samples and control samples (CS), as well as between urban and rural samples. For that purpose, a factor analysis of mixed data (FAMD) [56] was conducted on the quantitative reduced-centric data for the 45 compounds presenting a $Q_f > 0.6$, and on the qualitative 15 compounds having a Q_f between 0.3 and 0.6. Since the quantitative variables Ca, K, Mg, and Na were highly correlated with Ca^{2+} , K^+ , Mg^{2+} , and Na^+ , we calculated the difference for each of those variables with Ca^{2+} , K^+ , Mg^{2+} , and Na^+ , respectively, and retained their refractory component values (diff-Ca, diff-K, diff-Mg, diff-Na) for the FAMD analysis. The latter was followed by a hierarchical clustering on the factors obtained consolidated by a k-means [57] using the corresponding R package [58].

To identify the chemical profile of PM₁₀ during NADE, an orthogonal partial least squares discriminant analysis (OPLS-DA) was conducted [59] using the R package *Ropls* [60]. This method is particularly well adapted to quantitative data for which the number of variables studied is much higher than the number of observations and for which there is correlation between the variables. The OPLS-DA constructs a series of orthogonal com-

ponents between them in order to best predict the sample's affiliation group. The first component of the model is the predictive component (between-group variability) while the others are the non-correlated components (intra-group variability). This analysis is actually a partial least square (PLS) regression in which the response variable Y is a categorical one that expresses the class to which the observations belong. This qualitative variable Y with q classes is transformed into q dummy variables before running the PLS regression algorithm. PLS regression proceeds in successive steps in order to find H orthogonal components t_h and H u_h components well-correlated. The VIP criterion (Variable Importance in the Projection) is used to select the most discriminating explanatory variables. For p explanatory variables, the VIP of a variable x_j on the component h is:

$$VIP_{hj} = \sqrt{\frac{p}{Rd(Y; t_1, \dots, t_h)} \sum_{l=1}^h Rd(Y; t_l) w_{lj}^2} \quad (1)$$

where:

- The weight w_{lj}^2 allows to measure the contribution of a variable x_j to the construction of the component t_l ;
- $Rd(Y; t_l) = \frac{1}{q} \sum_{k=1}^q cor^2(y_k, t_l)$ is the part of variance of Y explained by the component t_l .

All chemical compounds with a VIP on the first component greater than 1 were considered to discriminate between samples collected during a NADE or not (CS). For each of them, tests of Wilcoxon's signed ranks were performed to test the statistical significance of the differences in mean concentrations measured for samples collected during NADE vs. CS. For each NADE, the samples were matched by calculating a couple of mean concentration pairs (the first calculated on samples collected during all consecutive days of the NADE in consideration; the second on the corresponding CS). All the test p -values were adjusted [61].

3. Results

All hereafter statistical descriptive analyses (Sections 3.1–3.3) were applied to the dataset obtained from the 27 collected samples: 20 during NADEs (10 from the rural area and 10 from the urban area) and 7 used as controls samples (5 from the rural area and 2 from the urban area).

3.1. PM_{10} Volumetric Concentration Levels

Based on analysis of PM_{10} daily time series (2005–2016), an index was empirically derived from the 24-h mean values of PM_{10} to define days without or with NADE: I0 (no NADE) if $PM_{10} \leq 27 \mu\text{g}/\text{m}^3$, I1 (light NADE) if $27 < PM_{10} \leq 38 \mu\text{g}/\text{m}^3$, I2 (moderate NADE) if $38 < PM_{10} \leq 54 \mu\text{g}/\text{m}^3$, and I3 (intense NADE) if $PM_{10} > 54 \mu\text{g}/\text{m}^3$.

Out of NADE, the median value ($n = 7$) of PM_{10} was $18.9 \mu\text{g}/\text{m}^3$ (min 7.3–max 27). For moderate NADE ($n = 10$), it was $44.7 \mu\text{g}/\text{m}^3$ (min 38.6–max 52.3), and for intense NADE ($n = 10$), the median value was $78.5 \mu\text{g}/\text{m}^3$ (min 64.6–max 153.5) (Figure 2).

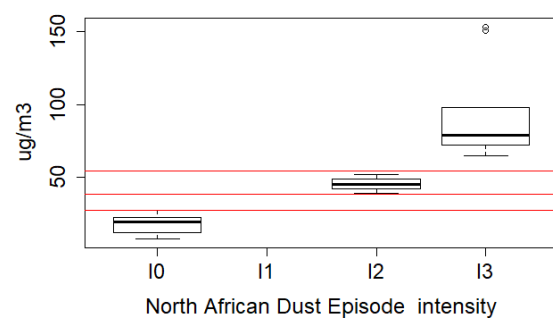


Figure 2. Box plots showing minimum, maximum, 75% and 25% percentiles, arithmetic median PM_{10} concentrations ($\mu\text{g}/\text{m}^3$) by NADE intensity (I), Guadeloupe, March–November 2017.

3.2. Dust Episodes Origin

NADE samples presented the following specific ratios: Ca/Al = 0.26 ± 0.02 , Ti/Fe = 0.07 ± 0.01 , Ti/Ca: 0.11 ± 0.01 , Fe/Al = 0.45 ± 0.01 and (Ca + Mg)/Fe = 1.07 ± 0.08 .

3.3. PM₁₀ Chemical Compounds Concentrations

Among the 51 elements analyzed, 17 (Al, As, Be, Ca, Ce, Cs, K, La, Li, Mg, Mn, Na, Rb, Se, Sr, Th, U) were quantified in all samples (NADE and CS), and 18 (Cd, Co, Cr, Dy, Er, Eu, Fe, Gd, Ho, Nd, Pb, Pr, Sb, Sc, Sm, Ti, Tl, V) were quantified with a Qf value between 0.6 and 1. Among the 57 organic compounds analyzed, only one (pyrene) was quantified with a frequency > 0.6. Among the 11 carbon compounds-anions-cations, 8 (Ca²⁺, Cl⁻, levoglucosan, NO³⁻, OC, K⁺, Na⁺, SO₄²⁻) were quantified in all samples (NADE and CS) and 1 (Mg²⁺) with a Qf > 0.6. Table 2 shows the concentrations in µg/g for those 45 compounds (Qf > 0.6), in NADE and CS (for compounds with a Qf < 0.6 see Table S3).

Table 2. Statistics for elements, organic compounds (particulate phase), and carbon-anions-cations PM₁₀ concentration (µg/g) with a Qf > 0.6, depending on collection conditions (20 NADEs vs. 7 controls), Guadeloupe, March—November 2017.

Elements/ Compounds	QL (µg/m ³)	Quantification Frequency	NADE Samples		Control Samples	
			Mean (µg/g)	SD	Mean (µg/g)	SD
Al	3.57×10^{-2}	100%	90,252.27	14,136.24	44,188.46	23,944.78
As	1.39×10^{-5}	100%	8.34	1.82	7.56	5.41
Be	0	100%	2.66	0.40	1.32	0.62
Ca	2.42×10^{-2}	100%	23,114.09	2386.32	24,678.60	9625.29
Cd	1.39×10^{-5}	78%	0.67	1.05	0.38	0.36
Ce	2.78×10^{-5}	100%	105.71	17.79	46.74	23.24
Co	2.22×10^{-4}	78%	14.64	2.35	8.92	3.42
Cr	2.40×10^{-3}	63%	61.59	13.90	89.37	42.37
Cs	0	100%	3.33	0.50	1.46	0.69
Dy	4.17×10^{-5}	74%	2.85	0.54	1.76	0.83
Er	2.78×10^{-5}	78%	1.25	0.32	0.93	0.36
Eu	2.78×10^{-5}	70%	0.92	0.22	0.93	0.44
Fe	4.13×10^{-2}	96%	40,288.33	6124.16	19,361.05	9900.01
Gd	4.17×10^{-5}	78%	3.69	0.88	1.94	0.74
Ho	1.39×10^{-5}	63%	0.48	0.15	0.62	0.29
K	4.38×10^{-2}	100%	17,381.37	1534.32	14,180.03	4339.40
La	1.39×10^{-5}	100%	45.74	7.72	20.03	10.02
Li	2.78×10^{-5}	100%	34.10	5.24	16.56	5.75
Mg	6.68×10^{-3}	100%	18,980.01	2201.94	21,130.22	6819.53
Mn	6.11×10^{-4}	100%	565.92	99.12	280.87	122.59
Na	1.45×10^{-2}	100%	71,620.49	21,043.91	161,142.72	92,117.83
Nd	9.72×10^{-5}	96%	18.62	3.83	9.02	3.52
Pb	1.53×10^{-4}	93%	28.85	7.90	13.75	5.41
Pr	2.78×10^{-5}	89%	4.97	1.01	2.15	1.23
Rb	2.78×10^{-5}	100%	79.73	11.44	37.11	15.22
Sb	1.11×10^{-4}	78%	11.39	21.67	6.48	4.30
Sc	2.78×10^{-5}	96%	12.29	2.05	5.56	2.95
Se	2.78×10^{-5}	100%	7.51	1.88	17.94	18.15
Sm	1.25×10^{-4}	67%	4.08	1.00	4.65	2.20
Sr	2.36×10^{-4}	100%	226.88	27.68	161.09	47.00
Th	1.39×10^{-5}	100%	13.58	2.11	5.83	2.90
Ti	7.57×10^{-3}	96%	2633.86	459.25	2153.32	1074.86
Tl	1.39×10^{-5}	74%	0.44	0.07	0.41	0.17
U	0	100%	2.45	0.28	1.20	0.53
V	2.50×10^{-4}	96%	110.63	32.89	56.66	25.59
Pyrene	5.33×10^{-6}	63%	0.27	0.32	1.08	1.33

Table 2. Cont.

Elements/ Compounds	QL ($\mu\text{g}/\text{m}^3$)	Quantification Frequency	NADE Samples		Control Samples	
			Mean ($\mu\text{g}/\text{g}$)	SD	Mean ($\mu\text{g}/\text{g}$)	SD
Ca ²⁺	3.90×10^{-2}	100%	14,792.37	1341.21	12 312.84	1706.38
Cl ⁻	1.50×10^{-2}	100%	75,678.27	24,237.95	157,701.21	65,400.07
Levogluconan	6.00×10^{-3}	100%	603.94	579.42	1563.14	1080.73
Mg ²⁺	1.50×10^{-2}	96%	5610.98	1718.57	8904.72	5253.78
NO ₃ ⁻	9.00×10^{-3}	100%	13,079.30	3808.51	12,053.54	5694.35
OC	1.29×10^{-1}	100%	19,859.47	11,469.10	51,105.19	29,056.23
K ⁺	3.90×10^{-2}	100%	2953.52	641.78	4925.05	1632.93
Na ⁺	5.10×10^{-2}	100%	48,838.48	15,847.95	103,154.76	39,641.48
SO ₄ ²⁻	1.50×10^{-2}	100%	33,658.63	7851.19	46,044.73	7479.11

Abbreviations: QL: Quantification limit; Qf: Quantification frequency; NADEs: North African dust event samples; SD: Standard deviation.

3.4. Chemical Profile of NADE PM₁₀

The hierarchical clustering consolidated by a k-means, performed on factors obtained after FAMD (after excluding a CS outlier), allows a clear distinction between control and NADE samples (Figure 3).

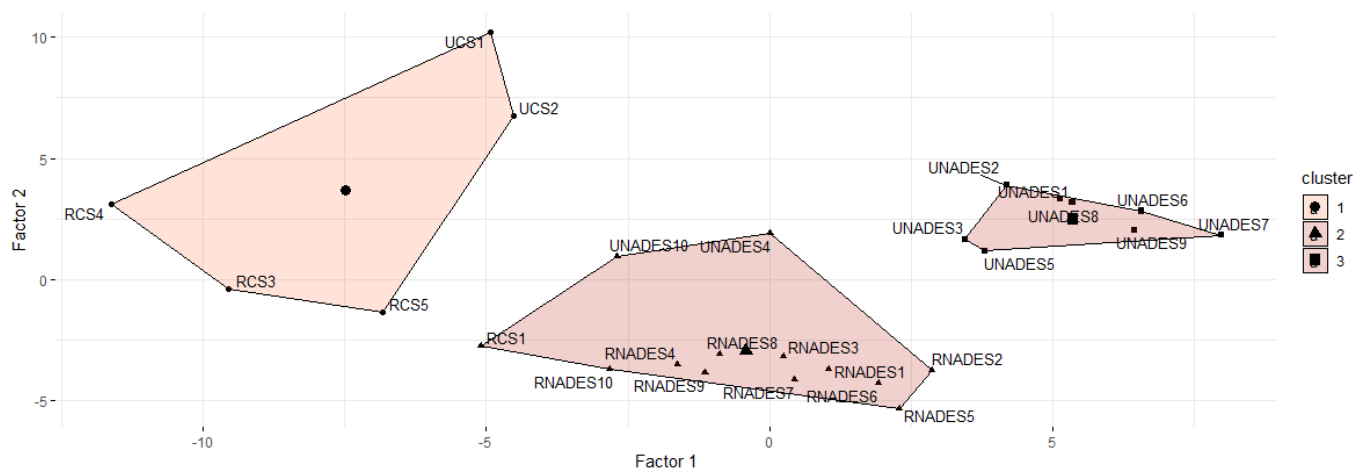


Figure 3. Results of a hierarchical clustering, consolidated by a k-means, conducted on factors obtained after factor analysis of mixed data on 26 PM₁₀ samples, Guadeloupe, 20. Abbreviations: UCS = Urban Control Sample; RCS = Rural Control Sample; UNADE = Urban North African Dust Event; RNADE = Rural North African Dust Event.

Samples taken in the rural area are also distinguished from those taken in the urban area. This classification identifies three clusters: One grouping, 5 of the 6 CS; another grouping, 8 of the 10 samples collected in the urban area during a NADE; and the last grouping, 10 samples collected in the rural area during a NADE, as well as 2 samples collected during a NADE in the urban area and the 6th control (rural) sample. This last sample being characterized by an average 24-h PM₁₀ value strictly equal to $27 \mu\text{g}/\text{m}^3$, we requalified it as a rural NADE sample of low intensity for further data analysis. The two urban NADE samples (UNADES4, UNADES10) are rather atypical, positioning themselves more or less in the center of the factorial plan, at distance from the other urban NADE samples. Although classified with rural NADE samples by the classification process, they are still quite distant from them.

The characteristic variables of each of these three clusters provided a first picture of the chemical compounds discriminating NADE samples from CS, as well as urban from rural samples. The CS cluster is mainly characterized by higher than means levels for Cr, Se, OC, diff-Cl, SO₄²⁻, diff-Na, levogluconan, and pyrene. Samples from the rural NADE cluster are characterized by higher than overall mean concentrations for the elements Sr,

diff-Mg, and PAH compounds are less frequently detected in samples from this cluster than in all samples. The urban NADE cluster is characterized by levels higher than overall mean concentrations for Al, Be, Ce, Cd, Co, Cs, Dy, Er, Eu, Fe, Gd, La, Mn, Nd, Pb, Pr, Th, U, Rb, Sb, Sc, Ti, V, NO_3^- , diff-K, and PAH compounds (benzo[a]anthracene, benzo[a]pyrene, benzo[b]fluoranthene, benzo[e]pyrene, benzo[g,h,i]perylene, benzo[k]fluoranthene, chrysene, coronene, fluoranthene, indeno[1,2,3-cd]pyrene, and retene) more frequently detected in samples from this cluster than in all samples. Therefore, the OPLS-DA analysis was applied to the modified dataset resulting from the re-qualification of one of the rural control sample as a rural NADE sample. It confirmed the existence of a difference in chemical composition (Figure 4), essentially observed between groups (NADE and CS); 77% of the data inertia being represented by the first component. It also confirms through the second component the FAMD analysis results, with a greater dispersion within the CS, vs. a lower dispersion in the samples taken during an NADE, respectively, in rural and urban areas.

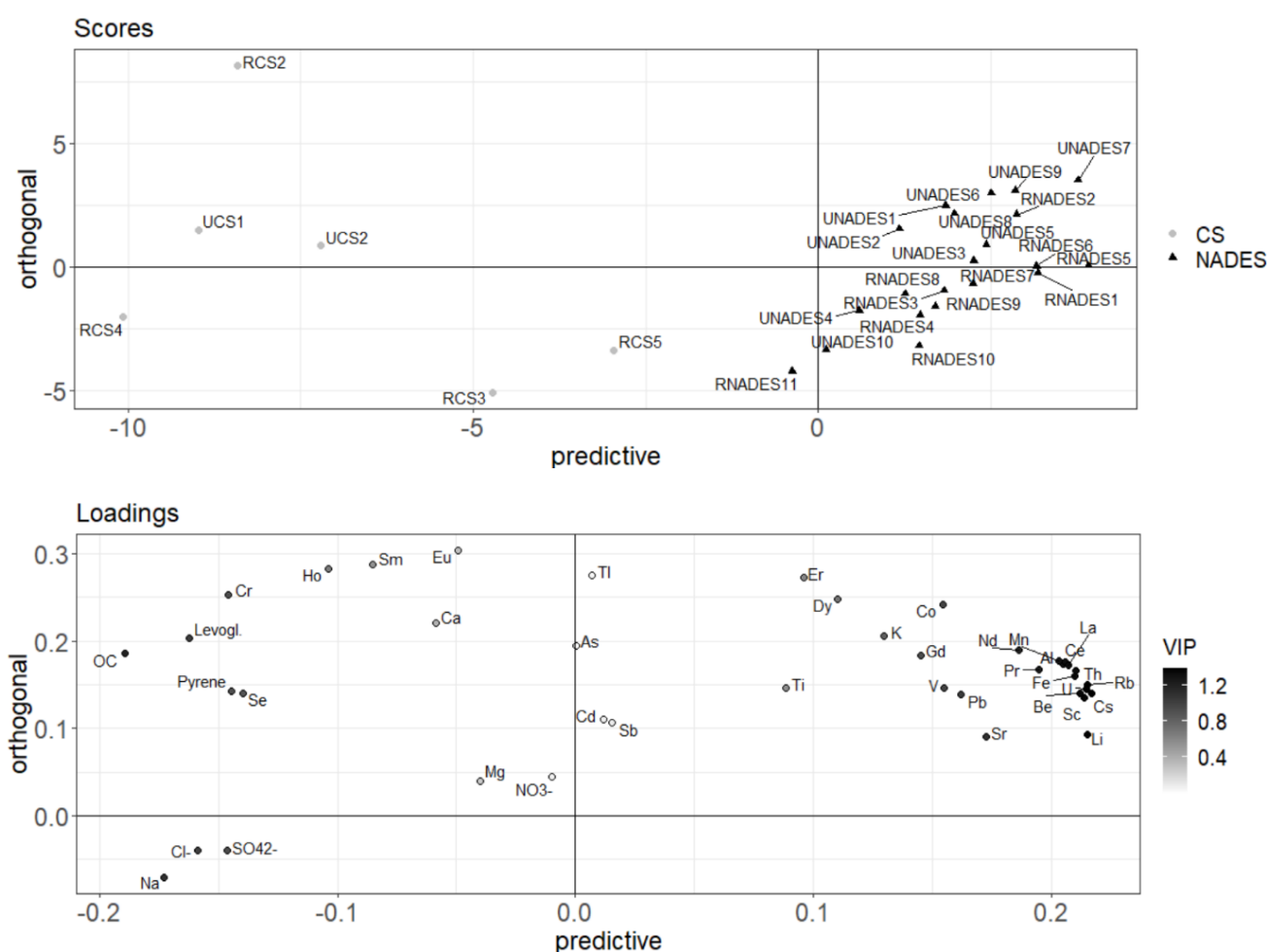


Figure 4. Results (scores and loadings scatter plots) of orthogonal partial least square discriminant analysis (OPLS-DA) on 27 PM_{10} samples, Guadeloupe, 2017.

Using the VIP criterion, 21 chemical compounds were identified as the most discriminant between the control and NADE samples (Figure 4): 16 elements (Al, Be, Ce, Cs, Fe, La, Li, Mn, Nd, Pb, Pr, Rb, Sc, Th, U, and V) with mass concentration levels about twice as high during a NADE compared to a CS, and 5 species (Cl^- , levoglucosan, OC, Na, and SO_4^{2-}) with levels about 2 to 3 times lower (Table 3). Wilcoxon tests allowed concluding that there was a statistically significant difference in concentration levels, with adjusted p -values below 5% for all compounds (Table 3).

Table 3. Mean values of elements in PM₁₀ characteristic (VIP > 1) of 21 NADE in Guadeloupe, 2017.

Caption Compounds	NADE Samples		Control Samples		Wilcoxon Tests Adjusted p-Value
	Mean (ug/g)	Mean (ng/m ³)	Mean (ug/g)	Mean (ng/m ³)	
Al	89,176.94	6059.01	40,274.79	585.88	3.42×10^{-2}
Be	2.63	0.18	1.19	0.02	3.42×10^{-2}
Ce	103.87	7.07	43.35	0.65	3.42×10^{-2}
Cs	3.27	0.23	1.36	0.02	3.42×10^{-2}
Fe	39,844.56	2711.32	17,426.35	263.88	3.42×10^{-2}
La	44.94	3.06	18.57	0.28	3.42×10^{-2}
Li	33.55	2.35	15.57	0.23	3.42×10^{-2}
Mn	558.68	37.98	258.73	3.90	3.42×10^{-2}
Nd	18.31	1.25	8.52	0.13	3.42×10^{-2}
Pb	28.16	1.87	13.64	0.22	3.42×10^{-2}
Pr	4.91	0.33	1.90	0.03	3.42×10^{-2}
Rb	78.32	5.42	34.96	0.53	3.42×10^{-2}
Sc	12.20	0.84	4.77	0.07	3.42×10^{-2}
Th	13.32	0.91	5.44	0.08	3.42×10^{-2}
U	2.41	0.16	1.13	0.02	3.42×10^{-2}
V	109.35	7.27	52.18	0.80	3.42×10^{-2}
Cl-	80,416.70	4901.43	154,787.22	2093.33	3.42×10^{-2}
Levogluconan	592.82	34.76	1761.94	25.00	3.42×10^{-2}
OC	19,707.43	1203.81	56,844.95	841.67	3.42×10^{-2}
Na	75,176.80	4656.87	163,616.00	2207.75	3.42×10^{-2}
SO ₄ ²⁻	34,366.24	2091.90	45,632.43	693.33	3.42×10^{-2}

Abbreviation: NADEs = North African Dust Event samples.

An OPLS-DA analysis (not shown) applied to samples collected only during NADE ($R^2 = 0.76$, $Q^2 = 0.62$) allows for a distinction between urban and rural samples. The first component being relatively low ($R^2 = 0.48$) suggests that the variability within NADE does not come solely from the sampling environment (rural vs. urban) as suggested by the value of the second component ($R^2 = 0.28$). It is probably related to the time difference between the two sampling periods at both stations, and it may also depend on the geographical origin of the NADE and/or its intensity.

4. Discussion

In 2017, five periods of dust events were investigated in Guadeloupe. During these events, the median PM₁₀ mass concentrations were on average 2 to 5 times and up to 10 times higher than in the post-episode baseline period (CS).

4.1. Origin of Particles

The mean elemental ratios of Ca/Al, Ti/Fe, Ti/Ca, Fe/Al and (Ca + Mg)/Fe measured during the NADE were somehow typical of what has been measured in the past. For instance, Remoundaki et al. [54] published comparable results for PM₁₀ collected at an urban site in Greece during an intense NADE when concentrations exceeded the daily EU limit value (50 $\mu\text{g}/\text{m}^3$). Interestingly, during these events, the concentrations of the mineral dust represented a large fraction of PM₁₀ reaching 79%. The Ti/Fe (0.08 ± 0.04) and Ti/Ca (0.03 ± 0.02) ratios reported by them were similar to those reported in the literature for long-range transported Saharan dust [62,63].

For Ca/Al ratios, the variability may be larger depending on the emission sources and Guieu and Thomas [64] found soil signatures around 0.28 and 0.36. Gelado-Caballero et al. [65] obtained Ca/Al ratios in aerosols collected in Gran Canaria, Canary Islands of 1.15 for Northern Sahara, 0.37 for West and Central Sahara and 0.43 for Sahel. Similarly, Formenti et al. [53] and Scheuven et al. [55] evidenced that on a regional scale, northern African dust and its source sediments are chemically heterogeneous which can be used to differentiate between major potential source areas. Consequently, using major elements ratios such as Ca/Al,

Mg/Al, Fe/Al, (Ca + Mg)/Fe may help to fingerprint Saharan dust source regions. Our results could suggest that the main origin of these events during the 2017 campaign carried out in Guadeloupe were partly coming from the so-called PSA-NAF3 at the Mali–Algerian border region [53] that display Fe/Al of 0.5–0.57 or (Ca + Mg)/Fe of 1.16–2.08.

4.2. Levels and Measurement of PM

Among the 20 NADE that occurred over five periods in Guadeloupe in 2017, half were of moderate intensity and the other half were of high intensity with an average value of almost $80 \mu\text{g}/\text{m}^3$ and a maximum level of $153 \mu\text{g}/\text{m}^3$. Many studies carried out in the Mediterranean basin have already shown an increase in PM_{10} concentrations during NADE, which can reach several hundred $\mu\text{g}/\text{m}^3$ [54,66,67]. In the Caribbean basin, due to the long distance travelled by the air masses, the PM_{10} levels are usually measured at lower levels; this was the case in our study where the levels measured were of the same order of magnitude as those already reported in studies conducted in the French West Indies [20,21].

In the Mediterranean basin, the rise in PM_{10} levels is mainly linked to an increase of the coarse fraction (larger than $\text{PM}_{2.5}$) and to a lesser extent in the finer fraction ($\text{PM}_{2.5}$) [54]. Moreover, about 50% of the dust of African origin correspond to particles with an aerodynamic diameter $\leq \text{PM}_{2.5}$ [7]; the mass median diameter of the particles being in the range 2.5 to $5.0 \mu\text{m}$ [68]. Knowing that $\text{PM}_{2.5}$ complements PM_{10} in WHO recommendations and in international or national regulations, it would have been interesting to also measure $\text{PM}_{2.5}$ in our study in order to compare the levels/enrichments of certain compounds that might have been slightly different. However, Perez et al. [12] showed that chemical composition varied equally in $\text{PM}_{2.5}$ and $\text{PM}_{10-2.5}$ during Saharan dust days over Spain. Moreover, the local monitoring network did not have yet the necessary equipment to measure the $\text{PM}_{2.5}$.

4.3. Chemical Composition of PM_{10}

Thanks to the complementarity of the analytical platforms and expertise between the three laboratories that performed the analysis, we were able to broadly explore the chemical composition of NADE PM_{10} particles. This investigation was based on a “suspect screening” approach considering the knowledge or hypotheses available in the literature regarding their composition and extended to a large set of elements and organic compounds ($n = 119$).

The objective of our study being to characterize qualitatively and quantitatively the specific chemical profile of PM_{10} during NADE using statistical modeling, we needed to use robust data. For this, we selected compounds with a value of QF > 0.6 allowing to select compounds with meaningful and robust means and SD values (below this threshold, the Qf were very low of the order of a few tens of %—see Table S3). Among the 51 elements and metalloids we analyzed, 35 were quantified with a value of Qf > 0.6 . Among them 16 (Al, Be, Ce, Cs, Fe, La, Li, Mn, Nd, Pb, Pr, Rb, Sc, Th, U and V) were identified as the most discriminant between the NADE and control samples. Although they have been found in significant quantities in mineral dust particles [23], Ca, K, or Na do not belong to this list. This can probably be explained by the fact that our study was conducted on an island territory where marine aerosols constitute an important source for these elements (the average contribution of sea salts to $\text{PM}_{10} = 13\%$ during NADE vs. 27% out of NADE).

Among the 57 organic compounds (organochlorines, organophosphorus compounds, oxadiazolones, phthalates, PCB, PAHs, and pyrethroids) we analyzed, only one (pyrene) was quantified with a frequency > 0.6 , with levels 4 times lower during NADE compared to control samples. Overall, compared to those observed in 2006 in the southeastern Caribbean region (Trinidad and Tobago) and in 2008 in the northeastern Caribbean (Virgin Islands) [24], the frequency of detection of SVOCs observed in our study (middle eastern Caribbean) is lower. The conservation of the samples at low temperature ($T < -20 \text{ }^\circ\text{C}$) all along the chain from sampling to analysis having been respected, these results can be explained by the fact that we only analyzed the particles collected on filters, whereas in Garrison’s

study [24] both particulate and gaseous phases were analyzed. However, for most of the SVOCs common to both studies, the results are very consistent. Indeed, during ADE as in our study, *o,p'*-DDD, *p,p'*-DDD, *o,p'*-DDE, *p,p'*-DDE, *o,p'*-DDT, *p,p'*-DDT, dieldrin, endosulfan sulfate, α -HCH, benzo(a)pyrene, PCB 101, PCB 118 and PCB 153 were detected by Garrison et al. with a low frequency (<0.6). On the other hand, as in our study, pyrene and fluoranthene were detected with a frequency of >0.55.

4.4. NADE PM₁₀ Profile

The only difference observed in our study concerning the chemical profile of PM₁₀ particles is related to their elemental composition, which varies in the order of two depending on whether they were collected during or out of NADE. We also observed a difference during NADE whether they were collected in urban or rural areas. However, due to the sampling time difference between these two sites, we were not able to demonstrate the origin of this dissimilarity. This is a limitation of our study due to the lack of human resources and material when the study was carried out.

The unsupervised statistical methods used to analyze our dataset allowed us to identify and compare to a baseline situation, a specific profile of 16 elements (Al, Be, Ce, Cs, Fe, La, Li, Mn, Nd, Pb, Pr, Rb, Sc, Th, U, and V) in the composition of NADE PM₁₀ (Figure 4). Indeed, the FAMD permitted to consider all the available information by applying a main component analysis on the quantitative variables ($n = 45$) and a multiple correspondence analysis on the qualitative variables ($n = 15$), enabling us to discriminate the PM₁₀ samples according to their overall composition. This was followed by an OPLS-DA model indicating the driving forces among the variables and which variables express this difference. Thanks to the large set of analyzed compounds and this multivariate approach, we characterized more extensively and specifically than before, the chemical profile of NADE PM₁₀.

However, our study focused on African dust probably originating from North Africa in the border region between Mali and Algeria, while African dust carried in the Atlantic Trade Winds derive from a wide range of sources in northern and western Africa [69]. The chemical properties of mineral dust can vary widely depending on the source and past history of the particles, preventing us to generalize our results to others NADE occurring in French West Indies. Nevertheless, as suggested by Prospero et al. [70], on a global scale, the major sources of NADE have a number of common features (locations in arid regions, topographical features, similar histories—the Pleistocene–Holocene boundary) suggesting that fine-grained dusts lifted from such sources might possess somewhat similar physical and chemical properties.

4.5. Health Risk Related to NADE PM₁₀

The PM₁₀ European directive has set a limit value for the 24-h average concentration of PM₁₀ less than 50 $\mu\text{g}/\text{m}^3$ with a tolerance of 35 exceedances per year to protect the human health [2]. The NADE PM₁₀ concentrations over the French West Indies are often at levels that challenge EU standards, and thus might raise health concerns. Indeed, in Guadeloupe, PM₁₀ EU standard levels were exceeded 25 times in 2005, 42 times in 2006, and 39 times in 2007 [71–73], the years during which pregnant women were enrolled in a previous epidemiological study we carried out [40]. In that study, we highlighted an association between mother's exposure to NADE during pregnancy and preterm birth; the exposure being assessed through two proxy indicators: (i) The frequency of exposure to intense NADE (i.e., PM₁₀ > 54 $\mu\text{g}/\text{m}^3$), and (ii) PM₁₀ levels. With these proxies, we observed an increase in relative risk (Odd ratio—OR) per standard deviation change (i.e., 4.06%) of the proportion of intense NADE, and for PM₁₀ concentrations per standard deviation (i.e., 3.08 $\mu\text{g}/\text{m}^3$), respectively OR = 1.54 (95% Confidence Interval 1.21 to 1.98) and OR = 1.40 (95% CI 1.08 to 1.81). These results are consistent too with the large number of recent publications suggesting that ambient air particulate matter pollution may play a role in preterm birth [74].

Nevertheless, the biological plausibility of this association remains to be documented. The fine characterization of the NADE PM₁₀ chemical profile we performed in our study is one of the key factors, with frequency, intensity, and duration in combination with physical activity, to assess the exposure of populations during the occurrence of NADE, and to explore the underlying biological pathways of the effect of particulate pollution on pregnancy. The latter are complex and multiple, but researchers have suggested the alteration of maternal–placental exchanges, oxidative pathways, and alteration of maternal host–defense systems as possible mechanisms [75]. In that perspective, is the NADE chemical profile observed in our study likely to constitute a risk exposure, and if so, to explain the epidemiological results related to preterm birth observed in Guadeloupe? In comparison to gaseous substances, the risk assessment of particulate elemental compounds as constituents of the aerosol is more difficult. This is due to the presence of a complex and variable mixture of chemical compounds with different toxic properties, a number of physicochemical factors such as water solubility, particle size distribution, and surface enrichment or encapsulation within the aerosol that can affect their bioavailability. Consequently, the assessment of effects related to elements' exposure is impaired by considerable uncertainties, and to date few substances have been assessed. The only ones for which recommendations and/or EU regulations have been issued in terms of target values not to be exceeded in ambient air in order to protect human health are Pb (250 ng/m³—annual mean), Ni (20 ng/m³—annual mean—for total nickel content in airborne dust), As (6 ng/m³—annual mean—for the total arsenic content in airborne dust), and Cd (5 ng/m³—annual mean—for the total cadmium content in airborne dust) [2].

Ni, As, and Cd do not belong to the elemental profile of NADE PM₁₀ in our study, and to date, no limit values in ambient air exist for the other elements identified belonging to this profile (Al, Be, Ce, Cs, Fe, La, Li, Mn, Pr, Rb, Sc, Th, U, and V). However, two of these (Mn and V) belong to the list of pollutants classified as emerging by the French Agency for Food, Environmental and Occupational Health and Safety [76] and will soon be subject to reinforce monitoring of their emissions. For other compounds, data on the associated health risks are scarce, in particular for exposure in the general population. As regards Al, one of the most studied compounds among the 14, the assessment of the associated health risks is facing difficulties, linked both to the assessment of aluminum exposure (inhalation is usually a minor route) and to the poor knowledge of the kinetics, metabolism, and toxicity of the different chemical forms of aluminum. Regarding Fe and V, the main route of exposure for the general population is the oral one through the ingestion of iron-vanadium containing food. Regarding Be, Ce, Fe, Li, Mn, Rb, Sc, and Th, most of the knowledge comes from studies conducted in workplaces or in the case of an accidental situation where exposures are high and where the hazards studied are mostly acute in nature [77,78]

Although the nature and precise exposure, and mechanisms underlying the effects of NADE particles revealed by epidemiological studies have yet to be elucidated, given the frequency with which these episodes occur (likely to increase with climate change), it is imperative that preventive measures are put in place to protect the population's health. In French West Indies, air quality monitoring networks and modeling tools now make it possible to predict the occurrence and intensity of these episodes and to detect them in real time. In the event of a pollution episode, it is advisable to act and protect the population. The response plan is based on three pillars: (i) Inform people via social networks or by email, (ii) reduce exposure avoiding intense physical and sports activities both outdoors and indoor and favoring shorter outings and those that require the least amount of effort, far from the main roads, and (iii) limit any further pollution indoor and outdoor. Although this response plan has been operational for more than 15 years, many questions systematically come to the forefront of the media during NADE, focusing on the risks for the health of the population. This study having provided an answer on the chemical profile of the particles observed in 2017, it is now necessary to set up a sampling plan for French West Indies (Guadeloupe and Martinique) and over (eastern Caribbean basin) to characterize the

possible different chemical profiles of the particles according to the origin of the NADE, and to complete these initial results. The results of our study call also for the implementation of prospective epidemiological studies (cohort studies) based on indicators of exposure to fine particles integrating their chemical composition, by adjusting the results for the place of habitual residence in order to take into account the risks associated with pollutants specific to the urban environment (PAHs) and collecting biomonitoring data enabling the study of biological pathways using omics methods.

5. Conclusions

Our study showed that the main chemical characteristic of particles of African origin coming potentially from the border region between Mali and Algeria and having exposed the Guadeloupean population to NADE in 2017, was their elemental composition with an almost total absence of SVOCs in the particulate phase. Among the 16 elements identified, knowledge of the hazards and associated risks are rare, and many are based on studies carried out in the workplace. These results call for further studies to be conducted in the Caribbean basin in order to provide answers to the extent and nature of exposure and health risks associated with NADE.

Supplementary Materials: The following are available online at <https://www.mdpi.com/2073-4433/12/2/277/s1>, Table S1: Statistics (mean, SD) for elements concentrations (ng/m³) of blanks filters and SRM measurements, Table S2: Statistics (mean, RSD) for concentrations of organic compounds other than PAHs in QC samples, Table S3: Statistics for elements, organic compounds (particulate phase) and carbon-anions-cations PM₁₀ concentration (µg/g) with a Q_f < 0.6, depending on collection conditions (20 NADEs vs. 7 controls), Guadeloupe, March–November 2017.

Author Contributions: Conceptualization, P.Q.; methodology, P.Q., C.G., and F.M.; validation, C.G., S.D., O.F., A.A., L.Y.A., and F.M.; formal analysis, J.V.; investigation, C.G., S.D., O.F., A.A., L.Y.A., and F.M.; resources, C.G., S.D., O.F., A.A., L.Y.A., and F.M.; data curation, J.V.; writing—original draft preparation, P.Q.; writing—review and editing, J.V., S.D., O.F., A.A., S.G., L.Y.A., and F.M.; visualization, J.V. and P.Q.; supervision, P.Q.; project administration, P.Q.; funding acquisition, P.Q., C.R. All authors have read and agreed to the published version of the manuscript.

Funding: This research was funded by the French National Research Program for Environmental and Occupational Health (PNR-EST) of the French Agency for Food, Environmental and Occupational Health & Safety (ANSES) (EST-2016/1/015); and by the French Ministry of Environment as part of the LCSQA (Central Laboratory of Air Quality Monitoring in France) activities.

Institutional Review Board Statement: Not applicable.

Informed Consent Statement: Not applicable.

Data Availability Statement: The data presented in this study are openly available in Mendely Data at <https://data.mendeley.com/datasets/rf4yvtmkvr/draft?a=d3957708-9a60-43ff-b0b6-8e4b56e237ad>.

Acknowledgments: We thank our partners of the BrumiSaTerre research group for fruitful discussions. The authors thank Gaëlle Saramito and Claude Briens at LERES for their contribution to the analysis of organic compounds and metals and metalloids respectively.

Conflicts of Interest: The authors declare no conflict of interest. The funders had no role in the design of the study; in the collection, analyses, or interpretation of data; in the writing of the manuscript, or in the decision to publish the results.

References

1. Taylor, D.A. Dust in the wind. *Environ. Health Perspect.* **2002**, *110*, A80–A87. [CrossRef]
2. EU (European Commission). Air Quality Standards. 2019. Available online: <https://ec.europa.eu/environment/air/quality/standards.htm> (accessed on 7 December 2020).
3. Prospero, J.M.; Bonatti, E.; Schubert, C.; Carlson, T.N. Dust in the Caribbean atmosphere traced to an African dust storm. *Earth Planet. Sci. Lett.* **1970**, *9*, 287–293. [CrossRef]
4. Prospero, J.M.; Glaccum, R.A.; Nees, R.T. Atmospheric transport of soil dust from Africa to South America. *Nat. Cell Biol.* **1981**, *289*, 570–572. [CrossRef]

5. Prospero, J.M. The Atmospheric Transport of Particles to the Ocean. In *Particle Flux in the Ocean*; Ittekkot, V., Schäfer, P., Honjo, S., Depetris, J., Eds.; John Wiley & Sons Ltd.: Berlin/Heidelberg, Germany, 1996; pp. 19–53.
6. Prospero, J.M.; Mayol-Bracero, O.L. Understanding the Transport and Impact of African Dust on the Caribbean Basin. *Bull. Am. Meteorol. Soc.* **2013**, *94*, 1329–1337. [[CrossRef](#)]
7. De Longueville, F.; Ozer, P.; Doumbia, S.; Henry, S. Desert dust impacts on human health: An alarming worldwide reality and a need for studies in West Africa. *Int. J. Biometeorol.* **2012**, *57*, 1–19. [[CrossRef](#)] [[PubMed](#)]
8. Goudie, A.S. Desert dust and human health disorders. *Environ. Int.* **2014**, *63*, 101–113. [[CrossRef](#)] [[PubMed](#)]
9. Sandstrom, T.; Forsberg, B. Desert Dust. *Epidemiology* **2008**, *19*, 808–809. [[CrossRef](#)] [[PubMed](#)]
10. Karanasiou, A.; Moreno, N.; Moreno, T.; Viana, M.; De Leeuw, F.; Querol, X. Health effects from Sahara dust episodes in Europe: Literature review and research gaps. *Environ. Int.* **2012**, *47*, 107–114. [[CrossRef](#)]
11. Stafoggia, M.; Zauli-Sajani, S.; Pey, J.; Samoli, E.; Alessandrini, E.; Basagaña, X.; Cernigliaro, A.; Chiusolo, M.; DeMaria, M.; Díaz, J.; et al. Desert Dust Outbreaks in Southern Europe: Contribution to Daily PM₁₀ Concentrations and Short-Term Associations with Mortality and Hospital Admissions. *Environ. Health Perspect.* **2016**, *124*, 413–419. [[CrossRef](#)]
12. Perez, L.; Tobias, A.; Querol, X.; Künzli, N.; Pey, J.; Alastuey, A.; Viana, M.; Valero, N.; González-Cabré, M.; Sunyer, J. Coarse Particles From Saharan Dust and Daily Mortality. *Epidemiology* **2008**, *19*, 800–807. [[CrossRef](#)] [[PubMed](#)]
13. Samoli, E.; Kougea, E.; Kassomenos, P.; Analitis, A.; Katsouyanni, K. Does the presence of desert dust modify the effect of PM₁₀ on mortality in Athens, Greece? *Sci. Total. Environ.* **2011**, *409*, 2049–2054. [[CrossRef](#)] [[PubMed](#)]
14. Sajani, S.Z.; Miglio, R.; Bonasoni, P.; Cristofanelli, P.; Marinoni, A.; Sartini, C.; Goldoni, C.A.; De Girolamo, G.; Lauriola, P. Saharan Dust Transport and Daily Mortality. *Epidemiology* **2009**, *20*, S40. [[CrossRef](#)]
15. Mallone, S.; Stafoggia, M.; Faustini, A.; Gobbi, S.; Forastiere, F.; A Perucci, C. Effect of Saharan Dust on the Association Between Particulate Matter and Daily Mortality in Rome, Italy. *Epidemiology* **2009**, *20*, S66–S67. [[CrossRef](#)]
16. Tobias, A.; Shahsavan, A.; Querol, X.; Stafoggia, M.; Hadei, M.; Hashemi, S.; Khosravi, A.; Namvar, Z.; Yarahmadi, M.; Emam, B. Short-term effects of desert dust and particulate matter on daily mortality in Iran. *Environ. Epidemiol.* **2019**, *3*, 396. [[CrossRef](#)]
17. Monteil, M.A. Saharan dust clouds and human health in the English-speaking Caribbean: What we know and don't know. *Environ. Geochem. Health* **2008**, *30*, 339–343. [[CrossRef](#)] [[PubMed](#)]
18. Prospero, J.M.; Blades, E.; Naidu, R.; Mathison, G.; Thani, H.; Lavoie, M.C. Relationship between African dust carried in the Atlantic trade winds and surges in pediatric asthma attendances in the Caribbean. *Int. J. Biometeorol.* **2008**, *52*, 823–832. [[CrossRef](#)] [[PubMed](#)]
19. Gyan, K.; Henry, W.; Lacaille, S.; Laloo, A.; Lamsee-Ebanks, C.; McKay, S.; Antoine, R.M.; Monteil, M.A. African dust clouds are associated with increased paediatric asthma accident and emergency admissions on the Caribbean island of Trinidad. *Int. J. Biometeorol.* **2005**, *49*, 371–376. [[CrossRef](#)] [[PubMed](#)]
20. Bateau, A.; Bouobda, D.; Le Tertre, A.; Gandar, S.; Quénel, P. Effets sanitaires des brumes de sable désertique à la Martinique, 2001–2006. *Bull. Veill. Sanit. Antilles-Guyane.* **2012**, *3*, 11–15. Available online: <https://www.santepubliquefrance.fr/regions/guyane/documents/bulletin-regional/2012/bulletin-de-veille-sanitaire-antilles-guyane-n-3-mars-2012> (accessed on 7 December 2020).
21. Cadelis, G.; Tourres, R.; Molinie, J. Short-Term Effects of the Particulate Pollutants Contained in Saharan Dust on the Visits of Children to the Emergency Department due to Asthmatic Conditions in Guadeloupe (French Archipelago of the Caribbean). *PLoS ONE* **2014**, *9*, e91136. [[CrossRef](#)]
22. Querol, X.; Alastuey, A.; Viana, M.; Rodriguez, S.; Artiñano, B.; Salvador, P.; Santos, S.G.D.; Patier, R.F.; Ruiz, C.; De La Rosa, J.; et al. Speciation and origin of PM₁₀ and PM_{2.5} in Spain. *J. Aerosol. Sci.* **2004**, *35*, 1151–1172. [[CrossRef](#)]
23. Artiñano, B.; Salvador, P.; Alonso, D.G.; Querol, X.; Alastuey, A. Anthropogenic and natural influence on the PM₁₀ and PM_{2.5} aerosol in Madrid (Spain). Analysis of high concentration episodes. *Environ. Pollut.* **2003**, *125*, 453–465. [[CrossRef](#)]
24. Garrison, V.; Majewski, M.; Foreman, W.; Genualdi, S.; Mohammed, A.; Simonich, S.M. Persistent organic contaminants in Saharan dust air masses in West Africa, Cape Verde and the eastern Caribbean. *Sci. Total. Environ.* **2014**, *468–469*, 530–543. [[CrossRef](#)] [[PubMed](#)]
25. Henn, B.C.; Ettinger, A.S.; Hopkins, M.R.; Jim, R.; Amarasiriwardena, C.; Christiani, D.C.; Coull, B.A.; Bellinger, D.C.; Wright, R.O. Prenatal Arsenic Exposure and Birth Outcomes among a Population Residing near a Mining-Related Superfund Site. *Environ. Health Perspect.* **2016**, *124*, 1308–1315. [[CrossRef](#)]
26. Davis, M.A.; Higgins, J.; Li, Z.; Gilbert-Diamond, D.; Baker, E.R.; Das, A.; Karagas, M.R. Preliminary analysis of in utero low-level arsenic exposure and fetal growth using biometric measurements extracted from fetal ultrasound reports. *Environ. Health* **2015**, *14*, 12. [[CrossRef](#)]
27. Ferguson, K.K.; Chin, H.B. Environmental Chemicals and Preterm Birth: Biological Mechanisms and the State of the Science. *Curr. Epidemiol. Rep.* **2017**, *4*, 56–71. [[CrossRef](#)] [[PubMed](#)]
28. Helmfrid, I.; Berglund, M.; Löfman, O.; Wingren, G. Health effects and exposure to polychlorinated biphenyls (PCBs) and metals in a contaminated community. *Environ. Int.* **2012**, *44*, 53–58. [[CrossRef](#)]
29. Menai, M.; Heude, B.; Slama, R.; Forhan, A.; Sahuquillo, J.; Charles, M.-A.; Yazbeck, C. Association between maternal blood cadmium during pregnancy and birth weight and the risk of fetal growth restriction: The EDEN mother–child cohort study. *Reprod. Toxicol.* **2012**, *34*, 622–627. [[CrossRef](#)]

30. Zhu, M.; Fitzgerald, E.F.; Gelberg, K.H.; Lin, S.; Druschel, C.M. Maternal Low-Level Lead Exposure and Fetal Growth. *Environ. Health Perspect.* **2010**, *118*, 1471–1475. [[CrossRef](#)]
31. Llanos, M.N.; Ronco, A.M. Fetal growth restriction is related to placental levels of cadmium, lead and arsenic but not with antioxidant activities. *Reprod. Toxicol.* **2009**, *27*, 88–92. [[CrossRef](#)]
32. Ferguson, K.K.; McElrath, T.F.; Meeker, J.D. Environmental Phthalate Exposure and Preterm Birth. *JAMA Pediatr.* **2014**, *168*, 61–67. [[CrossRef](#)] [[PubMed](#)]
33. Lenters, V.; Portengen, L.; Rignell-Hydbom, A.; Jönsson, B.A.; Lindh, C.H.; Piersma, A.H.; Toft, G.; Bonde, J.P.; Heederik, D.; Rylander, L.; et al. Prenatal Phthalate, Perfluoroalkyl Acid, and Organochlorine Exposures and Term Birth Weight in Three Birth Cohorts: Multi-Pollutant Models Based on Elastic Net Regression. *Environ. Health Perspect.* **2016**, *124*, 365–372. [[CrossRef](#)] [[PubMed](#)]
34. Chevrier, C.; Limon, G.; Monfort, C.; Rouget, F.; Garlandezec, R.; Petit, C.; Durand, G.; Cordier, S. Urinary Biomarkers of Prenatal Atrazine Exposure and Adverse Birth Outcomes in the PELAGIE Birth Cohort. *Environ. Health Perspect.* **2011**, *119*, 1034–1041. [[CrossRef](#)]
35. Kadhel, P.; Monfort, C.; Costet, N.; Rouget, F.; Thomé, J.-P.; Multigner, L.; Cordier, S. Chlordecone Exposure, Length of Gestation, and Risk of Preterm Birth. *Am. J. Epidemiol.* **2014**, *179*, 536–544. [[CrossRef](#)] [[PubMed](#)]
36. Kezios, K.L.; Liu, X.; Cirillo, P.M.; Cohn, B.A.; Kalantzi, O.I.; Wang, Y.; Petreas, M.X.; Park, J.-S.; Factor-Litvak, P. Dichlorodiphenyl-trichloroethane (DDT), DDT metabolites and pregnancy outcomes. *Reprod. Toxicol.* **2013**, *35*, 156–164. [[CrossRef](#)] [[PubMed](#)]
37. Longnecker, M.P.; Klebanoff, M.A.; Zhou, H.; Brock, J.W. Association between maternal serum concentration of the DDT metabolite DDE and preterm and small-for-gestational-age babies at birth. *Lancet* **2001**, *358*, 110–114. [[CrossRef](#)]
38. Taylor, P.R.; Lawrence, C.; Hwang, H.L.; Paulson, A.S. Polychlorinated biphenyls: Influence on birthweight and gestation. *Am. J. Public Health* **1984**, *74*, 1153–1154. [[CrossRef](#)]
39. Blondel, B.; Kermarrec, M. Enquête nationale périnatale 2010. In *Les Naissances en 2010 et leur Evolution Depuis 2003*; Inserm: Paris, France, 2011; pp. 3–47.
40. Viel, J.-F.; Mallet, Y.; Raghoumandan, C.; Quénel, P.; Kadhel, P.; Rouget, F.; Multigner, L. Impact of Saharan dust episodes on preterm births in Guadeloupe (French West Indies). *Occup. Environ. Med.* **2019**, *76*, 336–340. [[CrossRef](#)]
41. Westphal, D.L.; Curtis, C.A.; Liu, M.; Walker, A.L. Operational aerosol and dust storm forecasting. *IOP Conf. Ser. Earth Environ. Sci.* **2009**, *7*, 012007. [[CrossRef](#)]
42. EU (European Commission). Establishing Guidelines for Demonstration and Subtraction of Exceedances Attributable to Natural Sources under the Directive 2008/50/EC On Ambient Air Quality and Cleaner Air for Europe. 2008. Available online: https://ec.europa.eu/environment/air/quality/legislation/pdf/sec_2011_0208.pdf (accessed on 7 December 2020).
43. EU (European Commission). CSN EN 16450 Ambient air—Automated Measuring Systems for the Measurement of the Concentration of Particulate Matter (PM₁₀; PM_{2.5}). 2013. Available online: <https://www.en-standard.eu/csn-en-16450-ambient-air-automated-measuring-systems-for-the-measurement-of-the-concentration-of-particulate-matter-pm10-pm2-5/> (accessed on 7 December 2020).
44. Birch, M.E.; Cary, R.A. Elemental Carbon-Based Method for Monitoring Occupational Exposures to Particulate Diesel Exhaust. *Aerosol Sci. Technol.* **1996**, *25*, 221–241. [[CrossRef](#)]
45. Cavalli, F.; Viana, M.; Yttri, K.E.; Genberg, J.; Putaud, J.-P. Toward a standardised thermal-optical protocol for measuring atmospheric organic and elemental carbon: The EUSAAR protocol. *Atmospheric Meas. Tech.* **2010**, *3*, 79–89. [[CrossRef](#)]
46. Waked, A.; Favez, O.; Alleman, L.Y.; Piot, C.; Petit, J.-E.; Delaunay, T.; Verlinden, E.; Golly, B.; Besombes, J.-L.; Jaffrezo, J.-L.; et al. Source apportionment of PM₁₀ in a north-western Europe regional urban background site (Lens, France) using positive matrix factorization and including primary biogenic emissions. *Atmospheric Chem. Phys. Discuss.* **2014**, *14*, 3325–3346. [[CrossRef](#)]
47. EU (European Commission). EN 14902:2005 Ambient Air Quality—Standard Method for the Measurement of Pb, Cd, As, and Ni in the PM₁₀ Fraction of Suspended Particulate Matter. 2013. Available online: <https://infostore.saiglobal.com/preview/is/en/2005/i.s.en14902-2005%2Bac-2006.pdf?sku=675284> (accessed on 15 February 2021).
48. Mbengue, S.; Alleman, L.Y.; Flament, P. Size-distributed metallic elements in submicronic and ultrafine atmospheric particles from urban and industrial areas in northern France. *Atmospheric Res.* **2014**, *35*–47. [[CrossRef](#)]
49. Leclercq, B.; Alleman, L.Y.; Perdrix, E.; Riffault, V.; Happillon, M.; Strecker, A.; Lo-Guidice, J.-M.; Garçon, G.; Coddeville, P. Particulate metal bioaccessibility in physiological fluids and cell culture media: Toxicological perspectives. *Environ. Res.* **2017**, *156*, 148–157. [[CrossRef](#)] [[PubMed](#)]
50. Tomaz, S.; Shahpoury, P.; Jaffrezo, J.-L.; Lammel, G.; Perraudin, E.; Villenave, E.; Albinet, A. One-year study of polycyclic aromatic compounds at an urban site in Grenoble (France): Seasonal variations, gas/particle partitioning and cancer risk estimation. *Sci. Total. Environ.* **2016**, *565*, 1071–1083. [[CrossRef](#)] [[PubMed](#)]
51. Blanchard, O.; Glorennec, P.; Mercier, F.; Bonvallot, N.; Chevrier, C.; Ramalho, O.; Mandin, C.; Le Bot, B. Semivolatile Organic Compounds in Indoor Air and Settled Dust in 30 French Dwellings. *Environ. Sci. Technol.* **2014**, *48*, 3959–3969. [[CrossRef](#)]
52. Raffy, G.; Mercier, F.; Blanchard, O.; Derbez, M.; Dassonville, C.; Bonvallot, N.; Glorennec, P.; Le Bot, B. Semi-volatile organic compounds in the air and dust of 30 French schools: A pilot study. *Indoor Air* **2016**, *27*, 114–127. [[CrossRef](#)]

53. Formenti, P.; Schütz, L.; Balkanski, Y.; Desboeufs, K.; Ebert, M.; Kandler, K.; Petzold, A.; Scheuven, D.; Weinbruch, S.; Zhang, D. Recent progress in understanding physical and chemical properties of African and Asian mineral dust. *Atmospheric Chem. Phys. Discuss.* **2011**, *11*, 8231–8256. [[CrossRef](#)]
54. Remoundaki, E.; Bourliva, A.; Kokkalis, P.; Mamouri, R.-E.; Papayannis, A.; Grigoratos, T.; Samara, C.; Tsezos, M. PM₁₀ composition during an intense Saharan dust transport event over Athens (Greece). *Sci. Total. Environ.* **2011**, *409*, 4361–4372. [[CrossRef](#)]
55. Scheuven, D.; Schütz, L.; Kandler, K.; Ebert, M.; Weinbruch, S. Bulk composition of northern African dust and its source sediments—A compilation. *Earth Sci. Rev.* **2013**, *116*, 170–194. [[CrossRef](#)]
56. Pagès, J. Analyse factorielle de données mixtes. *Rev. Stat. Appl.* **2004**, *52*, 93–111.
57. Chen, B.; Harrison, R.; Pan, Y.; Tai, P.C. Novel Hybrid Hierarchical-K-means Clustering Method (H-K-means) for Microarray Analysis. In Proceedings of the 2005 IEEE Computational Systems Bioinformatics Conference-Workshops (CSBW'05), Stanford, CA, USA, 8–12 August 2006; IEEE: Piscataway, NJ, USA, 2006; pp. 105–108. [[CrossRef](#)]
58. Husson, F.; Josse, J.; Pagès, J. Principal Component Methods—Hierarchical Clustering—Partitional Clustering: Why Would We Need to Choose for Visualizing Data? Technical Report—Agrocampus. Applied Mathematics Department. September 2010. Available online: <http://www.agrocampus-ouest.fr/math/> (accessed on 15 February 2021).
59. Trygg, J.; Wold, S. Orthogonal projections to latent structures (O-PLS). *J. Chemom.* **2002**, *16*, 119–128. [[CrossRef](#)]
60. Thevenot, E.A. PCA, PLS(-DA) and OPLS(-DA) for Multivariate Analysis and Feature Selection of Omics Data. Bioconductor 3.12. Software Packages Ropls. Available online: <https://www.bioconductor.org/packages/release/bioc/html/ropls.html> (accessed on 15 February 2021).
61. Benjamini, Y.; Hochberg, Y. Controlling the false discovery rate: A practical and powerful approach to multiple hypothesis testing. *J. R. Stat. Soc.* **1995**, *57*, 289–300. [[CrossRef](#)]
62. Borbély-Kiss, I.; Kiss, Á.Z.; Koltay, E.; Szabó, G.; Bozó, L. Saharan dust episodes in Hungarian aerosol: Elemental signatures and transport trajectories. *J. Aerosol Sci.* **2004**, *35*, 1205–1224. [[CrossRef](#)]
63. Ganor, E.; Foner, H.A. The mineralogical and chemical properties and the behaviour of Aeolian Saharan dust over Israel. In *The Impact of Desert Dust across the Mediterranean*; Gurezoni, S., Chester, R., Eds.; Kluwer Academic Publishers: Dordrecht, The Netherlands, 1996; pp. 163–172.
64. Guieu, C.; Thomas, A.J. Saharan Aerosols: From the Soil to the Ocean. In *Environmental Science and Technology Library*; Springer: Berlin/Heidelberg, Germany, 1996; pp. 207–216.
65. Gelado-Caballero, M.D.; López-García, P.; Prieto, S.; Patey, M.D.; Collado, C.; Hernández-Brito, J.J. Long-term aerosol measurements in Gran Canaria, Canary Islands: Particle concentration, sources and elemental composition. *J. Geophys. Res. Space Phys.* **2012**, *117*, 03304. [[CrossRef](#)]
66. Koçak, M.; Mihalopoulos, N.; Kubilay, N. Contributions of natural sources to high PM₁₀ and PM_{2.5} events in the eastern Mediterranean. *Atmos. Environ.* **2007**, *41*, 3806–3818. [[CrossRef](#)]
67. Kleanthous, S.; Bari, A.; Baumbach, G.; Sarachage-Ruiz, L. Influence of particulate matter on the air quality situation in a mediterranean island. *Atmos. Environ.* **2009**, *43*, 4745–4753. [[CrossRef](#)]
68. Li-Jones, X.; Prospero, J.M. Variations in the size distribution of non-sea-salt sulfate aerosol in the marine boundary layer at Barbados: Impact of African dust. *J. Geophys. Res. Space Phys.* **1998**, *103*, 16073–16084. [[CrossRef](#)]
69. Prospero, J.M. African Droughts and Dust Transport to the Caribbean: Climate Change Implications. *Science* **2003**, *302*, 1024–1027. [[CrossRef](#)]
70. Prospero, J.M.; Ginoux, P.; Torres, O.; Nicholson, S.E.; Gill, T.E. Environmental characterization of global sources of atmospheric soil dust identified with the NIMBUS 7 Total Ozone Mapping Spectrometer (TOMS) absorbing aerosol product. *Rev. Geophys.* **2002**, *40*, 1002. [[CrossRef](#)]
71. Gwadair. Rapport d'Activité 2005. Available online: <https://www.gwadair.fr/images/pdf/rapport-activites2005.pdf> (accessed on 7 December 2020).
72. Gwadair. Rapport d'Activité 2006. Available online: <https://www.gwadair.fr/images/pdf/rapport-activites2006.pdf> (accessed on 7 December 2020).
73. Gwadair. Rapport d'Activité 2007. Available online: <http://www.gwadair.fr/images/pdf/rapport-activites2007.pdf> (accessed on 7 December 2020).
74. Zhao, N.; Qiu, J.; Zhang, Y.; He, X.; Zhou, M.; Li, M.; Xu, X.; Cui, H.; Lv, L.; Lin, X.; et al. Ambient air pollutant PM₁₀ and risk of preterm birth in Lanzhou, China. *Environ. Int.* **2015**, *76*, 71–77. [[CrossRef](#)] [[PubMed](#)]
75. Slama, R.; Darrow, L.; Parker, J.; Woodruff, T.J.; Strickland, M.; Nieuwenhuijsen, M.; Glinianaia, S.; Hoggatt, K.J.; Kannan, S.; Hurley, F.; et al. Meeting Report: Atmospheric Pollution and Human Reproduction. *Environ. Health Perspect.* **2008**, *116*, 791–798. [[CrossRef](#)] [[PubMed](#)]
76. ANSES. Polluants “Emergents” dans l’Air Ambiant: Identification, Catégorisation et Hiérarchisation de Polluants Actuellement non Réglementés pour la Surveillance de la Qualité de l’Air. Rapport d’Expertise Collective. 2018; pp. 1–250. Available online: <https://www.anses.fr/fr/system/files/AIR2015SA0216Ra.pdf> (accessed on 7 December 2020).

-
77. ANSES. Valeurs Limites d'Exposition en Milieu Professionnel: Evaluation des Indicateurs Biologiques d'Exposition et Recommandation de Valeurs Biologiques de Référence pour le Béryllium et ses Composés. 2018; pp. 1–75. Available online: <https://www.anses.fr/fr/system/files/VLEP2014SA0058Ra.pdf> (accessed on 7 December 2020).
 78. ANSES. Avis de l'Agence Nationale de Sécurité Sanitaire de l'Alimentation, de l'Environnement et du Travail Relatif à la Détermination d'une Valeur Sanitaire Maximale Admissible pour le Manganèse dans l'Eau Destinée à la Consommation Humaine Risques Professionnels. 2018; pp. 1–89. Available online: <https://www.anses.fr/fr/system/files/EAUX2016SA0203.pdf> (accessed on 7 December 2020).